Available online at www.sciencedirect.com
ScienceDirect
Remote Sensing of Environment 105 (2006) 189–203
Remote Sensing of Environment
www.elsevier.com/locate/rse

Characterization of seasonal variation of forest canopy in a temperate deciduous broadleaf forest, using daily MODIS data

Qingyuan Zhang [a,*,1], Xiangming Xiao [a], Bobby Braswell [a], Ernst Linder [b], Scott Ollinger [a], Marie-Louise Smith [c], Julian P. Jenkins [a], Fred Baret [d], Andrew D. Richardson [a], Berrien Moore III [a], Rakesh Minocha [c]

[a] *Institute for the Study of Earth, Oceans and Space, University of New Hampshire, Durham, NH 03824, USA*
[b] *Department of Mathematics and Statistics, University of New Hampshire, Durham, NH 03824, USA*
[c] *USDA Forest Service, Northeastern Research Station, P.O. Box 640 Durham, New Hampshire 03824, USA*
[d] *Institut National de la Recherche Agronomique, Site Agroparc, 84914 Avignon, France*

Received 2 December 2005; received in revised form 22 June 2006; accepted 22 June 2006

Abstract

In this paper, we present an improved procedure for collecting no or little atmosphere- and snow-contaminated observations from the Moderate Resolution Imaging Spectroradiometer (MODIS) sensor. The resultant time series of daily MODIS data of a temperate deciduous broadleaf forest (the Bartlett Experimental Forest) in 2004 show strong seasonal dynamics of surface reflectance of green, near infrared and shortwave infrared bands, and clearly delineate leaf phenology and length of plant growing season. We also estimate the fractions of photosynthetically active radiation (PAR) absorbed by vegetation canopy ($FAPAR_{canopy}$), leaf ($FAPAR_{leaf}$), and chlorophyll ($FAPAR_{chl}$), respectively, using a coupled leaf-canopy radiative transfer model (PROSAIL-2) and daily MODIS data. The Markov Chain Monte Carlo (MCMC) method (the Metropolis algorithm) is used for model inversion, which provides probability distributions of the retrieved variables. A two-step procedure is used to estimate the fractions of absorbed PAR: (1) to retrieve biophysical and biochemical variables from MODIS images using the PROSAIL-2 model; and (2) to calculate the fractions with the estimated model variables from the first step. Inversion and forward simulations of the PROSAIL-2 model are carried out for the temperate deciduous broadleaf forest during day of year (DOY) 184 to 201 in 2005. The reproduced reflectance values from the PROSAIL-2 model agree well with the observed MODIS reflectance for the five spectral bands (green, red, NIR_1, NIR_2, and $SWIR_1$). The estimated leaf area index, leaf dry matter, leaf chlorophyll content and $FAPAR_{canopy}$ values are close to field measurements at the site. The results also showed significant differences between $FAPAR_{canopy}$ and $FAPAR_{chl}$ at the site. Our results show that MODIS imagery provides important information on biophysical and biochemical variables at both leaf and canopy levels.

Keywords: Bartlett Experimental Forest; MODIS; Snow; Atmosphere contamination; Phenology; PROSPECT; SAIL-2; FAPAR; Markov Chain Monte Carlo (MCMC) method

1. Introduction

Seasonal variations of vegetation dynamics (e.g., leaf area index [LAI], fraction of photosynthetically active radiation [PAR] absorbed by vegetation canopy [$FAPAR_{canopy}$], and leaf phenology) have profound impacts on ecosystem fluxes of matter and energy, including carbon sinks and sources (Arora, 2002; Defries et al., 2002; Fitzjarrald et al., 2001; Lawrence & Slingo, 2004; Linderman et al., 2005; Osborne et al., 2004; Pielke et al., 1998; Zhang et al., 2004a). While the National

* Corresponding author. Complex Systems Research Center, Institute for the Study of Earth, Oceans and Space, University of New Hampshire, Durham, NH 03824, USA.
E-mail address: qyz72@yahoo.com (Q. Zhang).
[1] Now with Goddard Earth Science and Technology Center, University of Maryland Baltimore County, Baltimore, MD, 21228 and GSFC/NASA, Biospheric Sciences Branch, Code 614.4, Greenbelt, MD 20771, USA.

0034-4257/$ - see front matter © 2006 Elsevier Inc. All rights reserved.
doi:10.1016/j.rse.2006.06.013

Oceanic and Atmospheric Administration (NOAA) Advanced Very High Resolution Radiometer (AVHRR), particularly Normalized Difference Vegetation Index (NDVI, Tucker, 1979) of AVHRR, has been widely used to monitor long-term and/or large-scale vegetation trends, its inherent data and sensor problems and other noises limited its utility in change analyses in detail for short-terms, for example, daily, monthly or seasonally (Goward & Prince, 1995; Lovell & Graetz, 2001; Pettorelli et al., 2005; Prince & Goward, 1996).

The MODerate Imaging Spectrometer (MODIS) onboard Terra and Aqua satellites provides unprecedented data to monitor and quantify seasonal changes of forest canopy and phenology at local, regional and global scales. The MODIS science team provides standard products of LAI and $FPAR_{canopy}$ (note that it is also called $FAPAR_{canopy}$) (Knyazikhin et al., 1998a,b). The MODIS-based LAI and $FPAR_{canopy}$ at 1-km spatial resolution were generated by inversion of a radiative transfer model that uses surface reflectance of two bands (one red band and one near infrared band) or by an empirical model that describes the relationships among NDVI–LAI–$FPAR_{canopy}$ when there are not enough good-quality observations for inversion of the radiative transfer model. The retrieval algorithms are based on the assumption that leaf spectral properties for each biome type are constant (Myneni et al., 2002; Wang, 2002). Similarly, Gobron and colleagues assumed a single spectra profile for all leaves when they retrieved $FPAR_{canopy}$ (Gobron et al., 2000, 2002; Taberner et al., 2002).

However, many experiments showed that leaf structure and chemistry vary seasonally, resulting in seasonal dynamics of spectral properties. For example, some experiments showed that the chlorophyll concentration of leaves changed during the plant growing season (Demarez et al., 1999; Kodani et al., 2002). Another experiment also showed the variations of leaf water thickness and dry matter during the plant growing season (Gond et al., 1999). Accordingly, some researchers reported that their spectral measurements of leaves changed over the plant growing season (e.g., Demarez et al., 1999; Gitelson et al., 2002; Stylinski et al., 2002). Ustin, Duan and Hart documented the changes of the canopy reflectance of the grass vegetation, deciduous vegetation and evergreen vegetation over a plant growing season (Ustin et al., 1994). Kodani and colleagues documented the seasonal reflectance variation of Japanese beech from spring to autumn (Kodani et al., 2002), whereas Remer, Wald and Kaufman demonstrated changes in reflectance spectra of various ground surface targets, including forests, across three seasons (Remer et al., 2001). Work by Richardson and coauthors demonstrates that leaf reflectance properties change along elevational and latitudinal gradients; presumably this variation is driven by physiological differences resulting from differences in climate and site quality (Richardson & Berlyn, 2002; Richardson et al., 2003). So the seasonal and geographic variations of observed MODIS reflectance can be possibly attributed to variations of both canopy-level and leaf-level characteristics of vegetation.

The specific objectives of this study are threefold: (1) to develop an improved procedure that identifies snow-contaminated, atmosphere-contaminated or other poor quality observations in daily MODIS images; (2) to study the seasonal dynamics of surface reflectance and some widely used vegetation indices, using contamination-free-or-less MODIS time series data collection; and (3) to estimate LAI and the fractions of PAR absorbed by chlorophyll, leaf and canopy, i.e., $FAPAR_{canopy}$, $FAPAR_{leaf}$ and $FAPAR_{chl}$ with contamination-free multiple daily MODIS images. We used a coupled leaf-canopy radiative transfer model (PROSPECT model + SAIL-2 model; Zhang et al., 2005). Both the leaf-level PROSPECT model and canopy-level SAIL model have been discussed extensively in the published literature, both separately and in combination (Bacour et al., 2002; Baret & Fourty, 1997; Braswell et al., 1996; Combal et al., 2002; Di Bella et al., 2004; Gond et al., 1999; Jacquemoud & Baret, 1990; Jacquemoud et al., 1996, 2000; Kuusk, 1985; Verhoef, 1984, 1985; Verhoef & Bach, 2003; Weiss et al., 2000; Zarco-Tejada et al., 2003). Our coupled PROSPECT + SAIL-2 model (hereafter called PRO-SAIL-2 model) retrieves simultaneously both leaf-level variables and canopy-level variables (Zhang et al., 2005). As a case study, we selected a temperate deciduous broadleaf forest at the Bartlett Experimental Forest in the White Mountains of New Hampshire, USA, where field-based measurements of LAI, leaf dry matter, leaf chlorophyll content and $FAPAR_{canopy}$ are available for evaluating the inverted model variables.

2. Description of the study site and MODIS images

2.1. Brief description of the Bartlett Experimental Forest site

The Bartlett Experimental Forest eddy flux tower site (44.06°N, 71.29°W, 272 m elevation) is within the White Mountain National Forest in north central New Hampshire, USA. Established in 1932 as a USDA Forest Service research forest, the Bartlett Experimental Forest is a 1050 ha tract of secondary successional northern deciduous and mixed northern coniferous forest. The vegetation is primarily deciduous forest, dominated by American beech (*Fagus grandifolia*), yellow birch (*Betula alleghaniensis*), sugar maple (*Acer saccharum*), red maple (*Acer rubum*), paper birch (*Betula papyrifera*), white ash (*Fraxinus Americana*), and pin cherry (*Prunus pennsylvanica*). There are also some evergreen needleleaf species within the forest, for example, eastern hemlock (*Tsuga canadensis*), red spruce (*Picea rubens*), white pine (*Pinus strobus*) and balsam fir (*Abies balsamea*). Soils are mainly moist but well drained spodosols. The climate is warm in summer and cold in winter. Annual mean precipitation is about 127 cm, and the precipitation is distributed throughout the year. Winter snow can accumulate to the depths of 150 to 180 cm. Winter season covers from November to next May. Additional information of the study site is available elsewhere (Ollinger & Smith, 2005; http://www.fs.fed.us/ne/durham/4155/bartlett.htm#MPC).

The area surrounding the eddy flux tower site is relatively flat. Instruments to measure incident and canopy-reflected radiation (PPFD, LI-190 quantum sensor, Li-Cor Biosciences, Lincoln, NE; global radiation, CM-3 pyranometer, Kipp and Zonen, Delft, Netherlands) are located at the top of a 25 m eddy covariance flux tower. A below-canopy network of six quantum

sensors is located in a circle (radius = 15 m) around the base of the tower. Instruments are sampled every 10 s, and half-hourly means are output to a data logger (CR-10, Campbell Scientific, Logan, UT).

2.2. Brief description of daily MODIS images

MODIS daily surface reflectance (MOD09GHK and MYD09GHK, v004), MODIS daily observation viewing geometry (MODMGGAD and MYDMGGAD, v004), and MODIS daily observation pointers (MODPTHKM and MYDPTHKM, v004) are used in this study. The MODIS daily surface reflectance product at 500-m spatial resolution has reflectance values of the seven spectral bands: red (620–670 nm), blue (459–479 nm), green (545–565 nm), near infrared (NIR_1, 841–875 nm, and NIR_2, 1230–1250 nm), and short-wave infrared ($SWIR_1$, 1628–1652 nm, and $SWIR_2$, 2105–2155 nm). The MODIS daily observation viewing geometry product contains observation viewing geometry information (view zenith angle, view azimuth angle, sun zenith angle and sun azimuth angle) at a nominal 1-km scale. The MODIS daily observation pointers product provides a reference, at the 500 m scale, to observations that intersect each pixel of MODIS daily surface reflectance product in MODIS daily observation viewing geometry product (Zhang et al., 2005). All the MODIS data products are freely available at USGS Earth Observing System Data Gateway (http://edcimswww.cr.usgs.gov/pub/imswelcome/). The MODIS data are delivered to users in a tile fashion, each tile covering an area of 10° (latitude) and 10° (longitude).

We acquired daily MODIS data (tile H12V04) from the NASA data archive for an area containing the Bartlett Experimental Forest eddy flux tower site. Using the geolocation information of the eddy flux tower site, we extracted time series data of daily MODIS images for one MODIS pixel that centers on the flux tower site. All daily MODIS data in 2004 are used to study the seasonal dynamics of reflectance and phenology, and the daily MODIS data over date of year (DOY) of 184–201 in 2005 were used for inversion of the PROSAIL-2 model.

3. Method to identify snow- or atmosphere-contaminated MODIS daily observations

The MODIS daily surface reflectance product provides product quality information. Its quality control (QC) data layer includes information about errors and missing data in the daily surface reflectance product, for each of the seven MODIS bands, as well as information about whether an atmospheric correction was performed, and information about whether an adjacency correction was performed. If the QC value indicated any quality problem, the observation was not used in our analysis.

Furthermore, we examined reflectance values of $SWIR_2$ and blue bands for additional quality inspection. If one observation has $SWIR_2$ reflectance greater than 0.15 or blue reflectance greater than 0.2, the observation is identified as bad observation and excluded for analysis. Fig. 1a–b show the MODIS blue and $SWIR_2$ reflectance for those observations in 2004 with blue reflectance of ≤ 0.2 and $SWIR_2$ of ≤ 0.15. Some observations

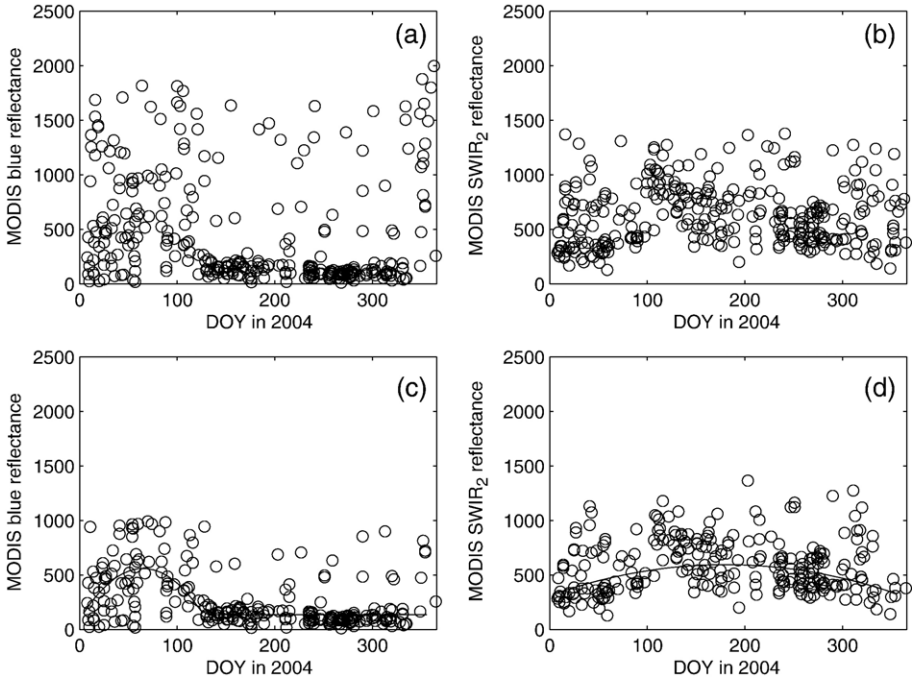

Fig. 1. Surface reflectance of blue and shortwave infrared ($SWIR_2$) bands of MODIS daily observations in 2004 for the Bartlett Experimental Forest tower site (reflectance scale = 0.0001). (a) and (b) for those observations with blue reflectance of < 0.2 and $SWIR_2$ reflectance of < 0.15; (c) and (d) for those observations with blue reflectance of < 0.1 and $SWIR_2$ reflectance of < 0.15.

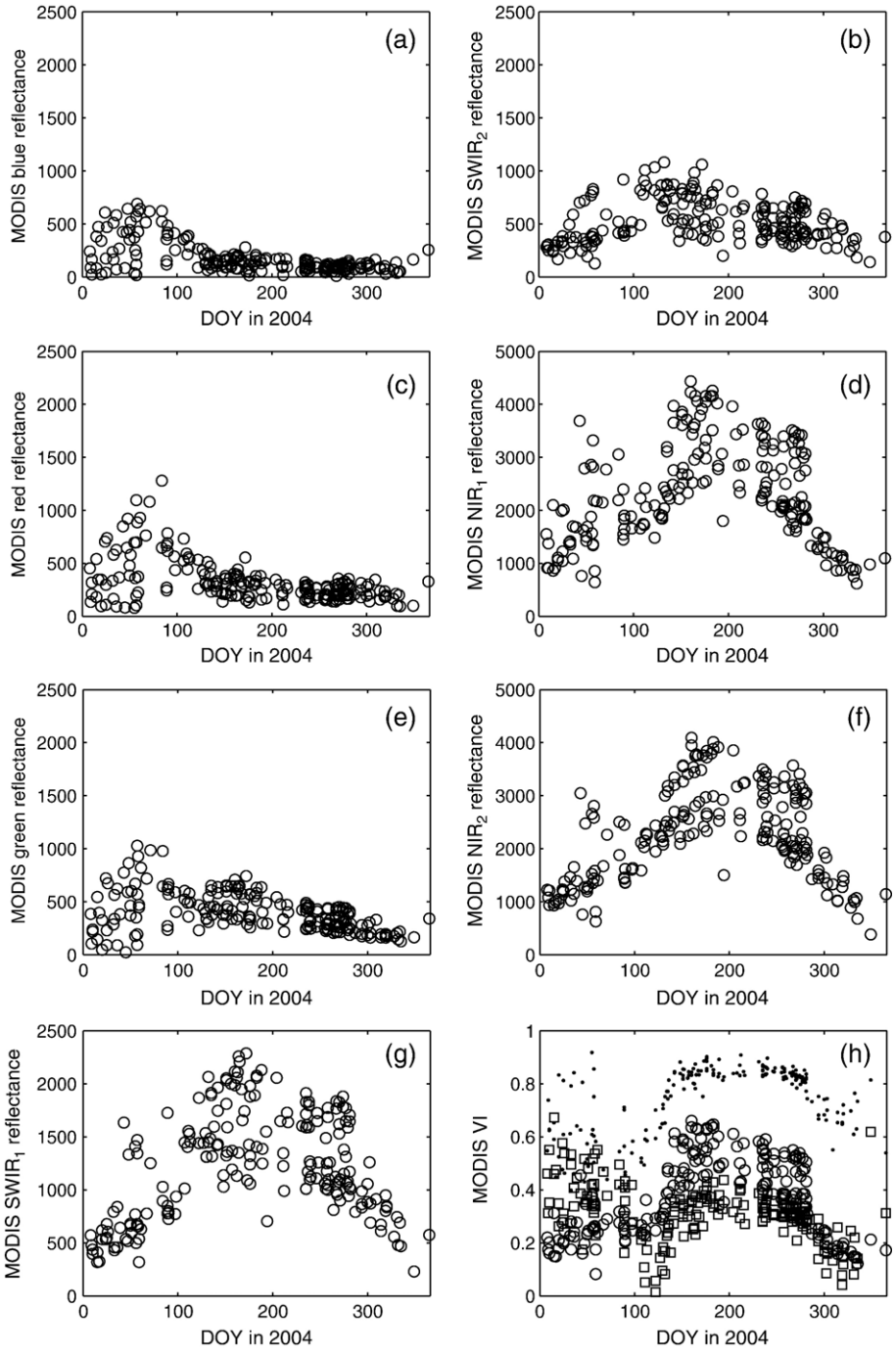

Fig. 2. Seasonal dynamics of surface reflectance and vegetation indices in 2004 at the Bartlett Experimental Forest tower site (reflectance scale=0.0001). Those observations with blue reflectance of <0.1 and $SWIR_2$ reflectance of <0.15 are presented here.

having both blue band ≤0.1 and $SWIR_2$ band ≤0.15 appear as clusters in Fig. 1c–d, while the other observations are randomly scattered. Contaminated atmosphere (e.g., partial cloud cover or residual aerosols) is one likely source that contributed to the scattering, though there are possibly other sources. We continued to remove those scattering observations, and Fig. 2 shows the reflectance of the MODIS seven bands for the remaining observations.

We calculated NDVI, Enhanced Vegetation Index (EVI, Huete et al., 1997), Land Surface Water Index (LSWI, Xiao et al., 2004), and snow cover fraction (f_{snow}, Kaufman et al., 2002) for those observations in Fig. 2a–g. The vegetation indices and snow cover fraction are shown in Figs. 2h and 3.

$$\mathrm{NDVI} = \frac{\rho_{\mathrm{NIR}_1} - \rho_{\mathrm{red}}}{\rho_{\mathrm{NIR}_1} + \rho_{\mathrm{red}}} \tag{1}$$

$$\mathrm{EVI} = 2.5 \times \frac{\rho_{\mathrm{NIR}_1} - \rho_{\mathrm{red}}}{\rho_{\mathrm{NIR}_1} + 6 \times \rho_{\mathrm{red}} - 7.5 \times \rho_{\mathrm{blue}} + 1} \tag{2}$$

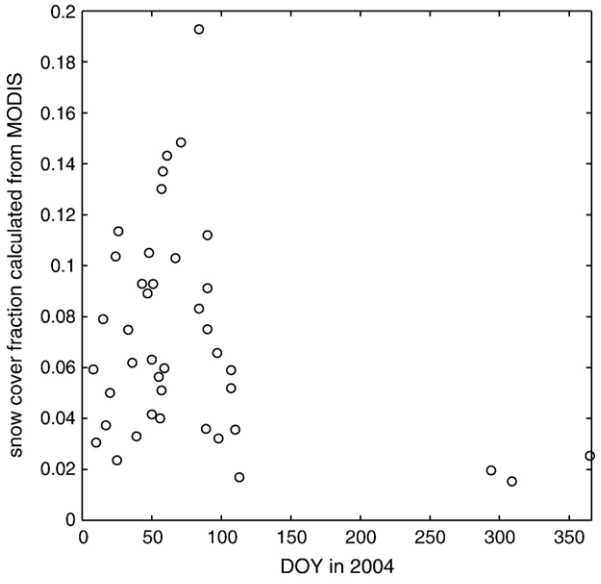

Fig. 3. Seasonal dynamics of snow cover fraction in 2004, as calculated from those MODIS daily observations with blue reflectance of <0.1 and $SWIR_2$ reflectance of <0.15.

$$\mathrm{LSWI} = \frac{\rho_{\mathrm{NIR}_1} - \rho_{\mathrm{SWIR}_1}}{\rho_{\mathrm{NIR}_1} + \rho_{\mathrm{SWIR}_1}} \tag{3}$$

$$f_{\mathrm{snow}} = \begin{cases} \dfrac{\frac{\rho_{\mathrm{red}} - 0.5\rho_{\mathrm{SWIR}_2}}{0.6}}{0.51 + 0.07 \times \frac{\rho_{\mathrm{red}} - 0.5\ \rho_{\mathrm{SWIR}_2}}{0.6}}, \text{if } \rho_{\mathrm{red}} > 0.5\ \rho_{\mathrm{SWIR}_2} \text{ and } \rho_{\mathrm{SWIR}_2} \le 0.15 \\ 0, \text{otherwise} \end{cases} \tag{4}$$

where ρ_{blue}, ρ_{red}, ρ_{NIR_1}, ρ_{SWIR_1} and ρ_{SWIR_2} are reflectance values of the blue, red, NIR_1, $SWIR_1$ and $SWIR_2$ bands. Fig. 4a–g showed the observations in Fig. 2a–g except the snow affected observations. Fig. 4h shows the NDVI, EVI and LSWI in Fig. 2h except the snow affected observations.

4. Brief description of the radiative transfer model and the inversion algorithm

We used the same PROSAIL-2 model as in our previous study (Zhang et al., 2005). Replacing leaf description in the canopy radiative transfer model – SAIL (Scattering from Arbitrarily Inclined Leaves) with the leaf radiative transfer model – PROSPECT is the way to couple. The SAIL model has an evolving history more than two decades with minor changes reflecting individual study objectives (e.g., Andrieu et al., 1997; Badhwar et al., 1985; Braswell et al., 1996; Goel & Deering, 1985; Goel & Thompson, 1984; Jacquemoud et al., 2000; Kuusk, 1985; Major et al., 1992; Verhoef, 1984, 1985). The version of SAIL model provided by Braswell and others (SAIL-2; Braswell et al., 1996) was used in this study. A vegetation canopy in the SAIL-2 model is decomposed into stems and leaves. In a typical parameterization, stems have spectral properties that are more similar to soil and litter than green leaves. Leaf and stem mean inclination angles, and the self-shading effect of both leaves and stems are also considered. The PROSPECT model we used has five variables: leaf internal structure variable (N), leaf chlorophyll content (C_{ab}), leaf dry matter content (C_{m}), leaf water thickness (C_{w}) and leaf brown pigment (C_{brown}) (Baret & Fourty, 1997; Di Bella et al., 2004; Verhoef & Bach, 2003). The brown pigment in the five-variable PROSPECT model is needed for light absorption by non-chlorophyll pigments in leaf. The coupled PROSAIL-2 model was used to describe optical characteristics (reflectance, absorption and transmittance) of the canopy and its components. The sixteen biophysical/biochemical variables of the PROSAIL-2 model (Table 1) are plant area index (PAI), stem fraction (SFRAC), cover fraction (CF), stem inclination angle (STINC), stem bidirectional reflectance distribution function (BRDF) effect variable (STHOT), leaf inclination angle (LFINC), leaf hot spot effect variable (LFHOT), five leaf variables that simulate leaf optical properties (N, C_{ab}, C_{m}, C_{w}, C_{brown}), two soil/litter variables that simulate soil/litter optical properties ($SOIL_A$, $SOIL_B$; Eq. (5)), and two stem variables that simulate stem optical properties ($STEM_A$, $STEM_B$; Eq. (6)). We assume the pixel covering the Bartlett Experimental Forest eddy flux tower site may include three parts: leaf, stem and soil (Braswell, 1996; Braswell et al., 1996; Qin, 1993). Cover fraction and stem fraction are used to address the decomposition. Because the MODIS data used in the study were atmospherically corrected, we do not consider atmospheric effect when we do inversion of the PROSAIL-2 model.

$$\rho_{\mathrm{soil}}(\lambda) = \frac{\mathrm{SOIL_A}}{1 + (10 \cdot \mathrm{SOIL_A} - 1) \cdot \exp\left(-\dfrac{\lambda - 400}{\mathrm{SOIL_B}}\right)}, \quad \text{where } \lambda \text{ is wavelength (nm)} \tag{5}$$

$$\rho_{\mathrm{stem}}(\lambda) = \frac{\mathrm{STEM_A}}{1 + (10 \cdot \mathrm{STEM_A} - 1) \cdot \exp\left(-\dfrac{\lambda - 400}{\mathrm{STEM_B}}\right)}, \quad \text{where } \lambda \text{ is wavelength (nm).} \tag{6}$$

A method based on the Metropolis algorithm (Braswell et al., 2005; Hurtt & Armstrong, 1996; Metropolis et al., 1953; Zhang et al., 2005) was employed for inversion using the MODIS data. Fig. 4 (a) shows that the MODIS blue reflectance over the site under cloud-free condition is less than 0.05 during plant growing season in 2004. There are thirteen observations for the period (DOY 184 to 201 in 2005) after discarding the observations with MODIS blue reflectance greater than 0.05. The thirteen observations are used for inversion. All mathematical description of the method can be found in the previous paper. The search ranges of the sixteen biophysical/ biochemical variables of the PROSAIL-2 model, based on an extensive literature review, were listed in Table 1. The prior distributions of the variables are uniform over the search ranges of the variables (Zhang et al., 2005). It is worthwhile to note that the spectral reflectance is dependent on both the sun-sensor-target geometry and spectral wavelength. The strength of the method is that it can estimate posterior probability distributions of the variables and thus the

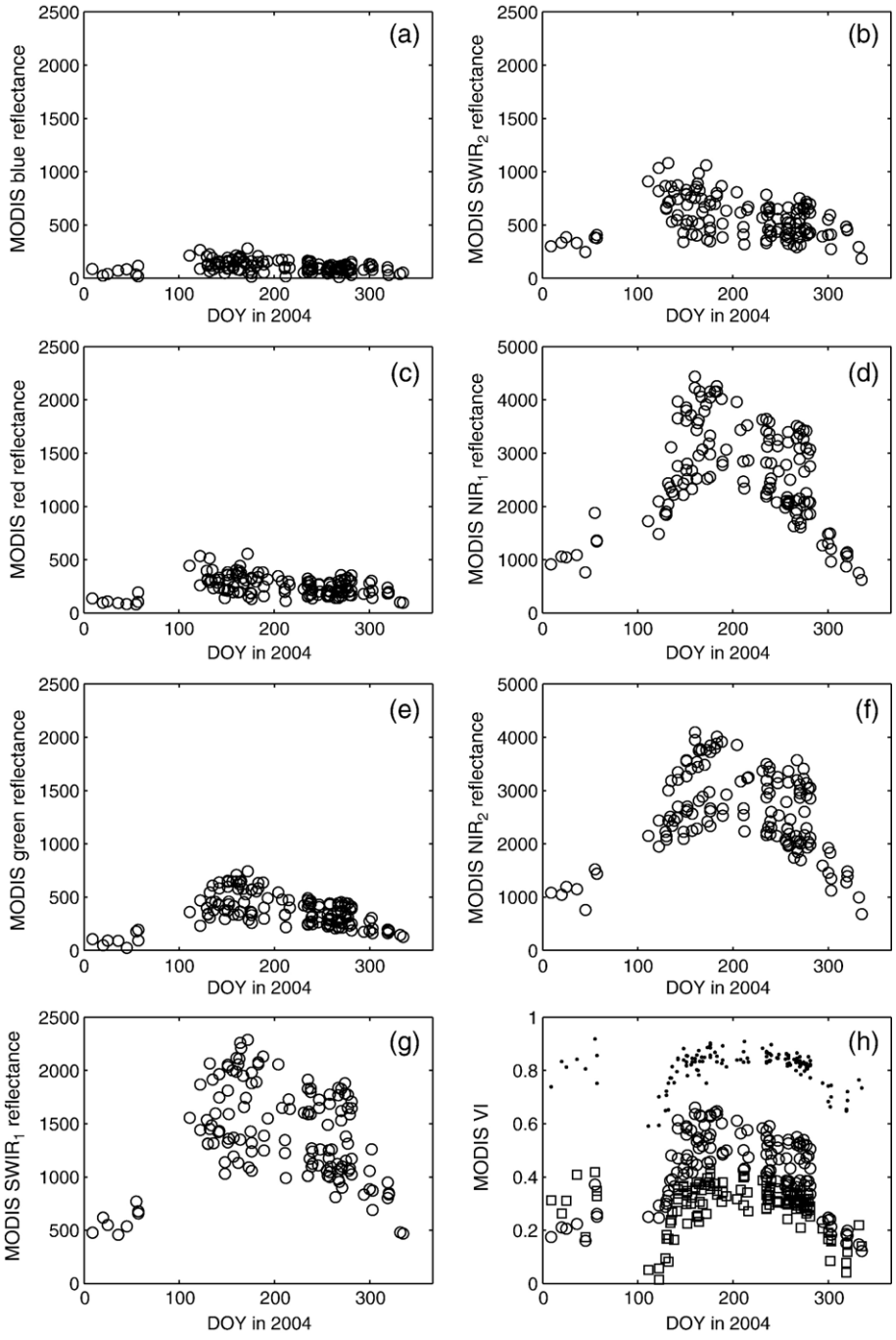

Fig. 4. Seasonal dynamics of surface reflectance and vegetation indices in 2004 at the Bartlett Experimental Forest tower site (reflectance scale = 0.0001), Those observations with no snow- and atmospheric-contamination are presented in the graph.

retrieved distributions can provide estimates of uncertainty (e.g., standard deviations and confidence intervals) of individual variables, conditioned on both the model and the observed data. The retrieved distributions can also provide information about the variable sensitivity of the model. The Metropolis algorithm is relatively computationally intensive, because of its need for simulation of a large number of samples to obtain a reliable estimate of the variables' distributions. It arises within a Bayesian statistical estimation framework (Gelman et al., 2000) and reflects the remaining uncertainty after the model has been constrained (inverted) with data. It constructs a random walk (Markov chain) through two steps: first at the current iteration, generating a new randomly generated "proposal" value, and secondly testing an acceptance as follows: if the posterior density increases, the proposed value is accepted, i.e. it becomes the new value of the random walk, if the posterior density decreases, the proposed value is only accepted with a probability equal to the ratio of the new value posterior density over current value posterior density. MODIS red, green, NIR_1, NIR_2 and $SWIR_1$ reflectance are used to calculate likelihood function. We also applied the same simulated annealing temperature adaptation as in our previous study (Zhang et al., 2005).

Table 1
A list of variables in the PROSAIL-2 model and their search ranges

Variable	Description	Unit	Search range
PAI	Plant area index, i.e., leaf + stem area index	m^2/m^2	1–7.5
SFRAC	Stem fraction		0–1
CF	Cover fraction: area of land covered by vegetation/total area of land		0.5–1
C_{ab}	Leaf chlorophyll a+b content	$\mu g/cm^2$	0–80
N	Leaf structure variable: measure of the internal structure of the leaf		1.0–4.5
C_w	Leaf equivalent water thickness	cm	0.001–0.15
C_m	Leaf dry matter content	g/cm^2	0.001–0.04
C_{brown}	Leaf brown pigment content		0.00001–8
LFINC	Mean leaf inclination angle	degree	10–89
STINC	Mean stem inclination angle	degree	10–89
LFHOT	Leaf BRDF variable: length of leaf/height of vegetation		0–0.9
STHOT	Stem BRDF variable: length of stem/height of vegetation		0–0.9
$STEM_A$	Stem reflectance variable: maximum (for a fitted function)		0.2–20
$STEM_B$	Stem reflectance variable range (for same fitted function)		50–5000
$SOIL_A$	Soil reflectance variable: maximum (for a fitted function)		0.2–20
$SOIL_B$	Soil reflectance variable: range (for same fitted function)		50–5000

We calculate $FAPAR_{canopy}$ (Goward & Huemmrich, 1992), $FAPAR_{leaf}$ (Braswell et al., 1996), and $FAPAR_{chl}$ (see Eqs. (7)–(11)) using the inverted biophysical and biochemical variables as input of PROSAIL-2 forward simulations.

$$FAPAR_{canopy} = \frac{APAR_{canopy}}{PAR_0} \quad (7)$$

$$FAPAR_{leaf} = \frac{APAR_{leaf}}{PAR_0} \quad (8)$$

$$FAPAR_{chl} = \frac{APAR_{chl}}{PAR_0} \quad (9)$$

$$APAR_{canopy} = APAR_{leaf} + APAR_{stem} \quad (10)$$

$$APAR_{leaf} = APAR_{chl} + APAR_{dry\ matter} + APAR_{brown\ pigment} \quad (11)$$

where PAR_0 is the incoming PAR at the top of the canopy, and APAR is the absorbed PAR. $APAR_{canopy}$, $APAR_{leaf}$, $APAR_{stem}$, $APAR_{chl}$, $APAR_{dry\ matter}$, and $APAR_{brown\ pigment}$ are absorbed PAR by canopy, leaf, stem, chlorophyll in leaf, dry matter in leaf, and brown pigment in leaf, respectively.

5. Results

5.1. Temporal analyses of MODIS daily reflectance data in 2004

Fig. 2 exhibits the time series of surface reflectance for the seven spectral bands among the atmospheric-contamination-free MODIS daily data that covered the Bartlett Experimental Forest flux tower site. The surface reflectance values of blue band for the period after DOY 122 are much lower than those for the period before DOY 122 (Fig. 2a). Similar seasonal patterns are also observed for surface reflectance in green and red bands (Fig. 2c, e). In comparison, surface reflectance values of NIR_1, NIR_2 and $SWIR_1$ bands have a strong seasonal dynamics with peak values in mid summer (Fig. 2d, f, g).

Higher surface reflectance values of visible bands (blue, green and red) in early part of the year suggest that snow cover occurs over that period and thus affects surface reflectance. There existed fractional snow cover through much of winter and early spring (Fig. 3) at the site. We further exclude those observations with a fractional snow cover and Fig. 4 shows the surface reflectance values of those observations without snow cover. Among the three visible bands, surface reflectance of green band has a distinct seasonal dynamics with peak values in late-June to early July (Fig. 4e).

The seasonal dynamics of surface reflectance of individual spectral bands provide rich information for interpreting vegetation indices from the MODIS data and understanding the impacts of snow cover on vegetation indices. Our analysis identifies those daily observations that were partially covered by snow (Fig. 3). The snow-covered season in 2004 for the study site ended around DOY 110. Without knowing information of both the fraction of snow cover and the surface reflectance over a MODIS pixel, one will have some difficulties in accurately interpreting NDVI, EVI and LSWI during the winter/spring seasons. There is very little green vegetation for the periods of DOY 1–100 and DOY 300–365 (Fig. 4d). However, many observations in the winter/spring seasons still have high NDVI values, for example, one MODIS observation on DOY 57 has NDVI value of 0.856 (Fig. 2h). The high NDVI values in the winter/spring seasons are likely attributed to both the wetness of soil/canopy background and the higher solar zenith angles in winter/spring seasons (in comparison to solar zenith angles in summer/autumn). Note that $SWIR_2$ reflectance was low during the winter/spring seasons, which clearly suggests a wet soil/canopy background in that period. Moderate LSWI values in that period also suggest a wet soil/canopy background. The NIR_1 reflectance was low during the period, which suggests that there is little green vegetation during the period. Observations of bare or sparse vegetation targets with higher solar zenith angles could result in higher NDVI values than observations of same targets with lower solar zenith angles (Goward & Huemmrich, 1992; Huete et al., 1992). Although the NIR_1 reflectance was low during the same period, reflectance values of blue, green, and red bands were much smaller than NIR_1 reflectance (Fig. 4a, c, d, and e). As a result, the mathematic formulation of NDVI still gives high NDVI values for some observations in the winter/spring seasons. This is consistent with earlier studies that examined the impacts of soil background and solar-view geometry on NDVI (Huete et al., 1997). Caution should be taken when using only NDVI to monitor vegetation phenology because NDVI is very sensitive to soil/canopy background wetness and solar-view geometry when green vegetation cover fraction is small.

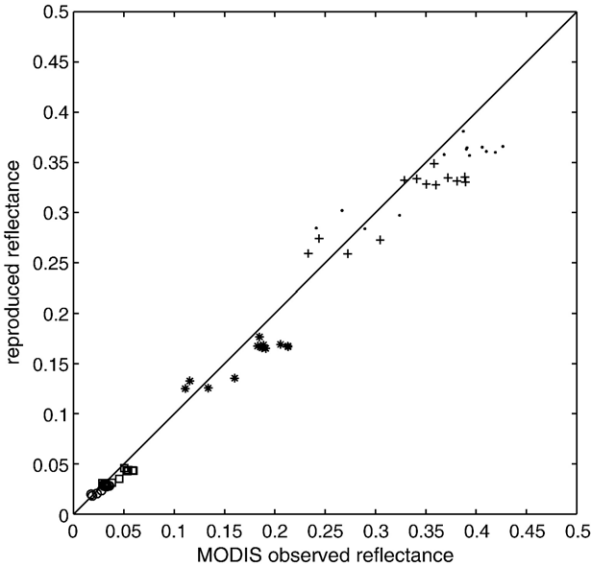

Fig. 5. A comparison between the observed reflectance and PROSAIL-2 estimated reflectance for five MODIS spectral bands (red, green, NIR_1, NIR_2 and $SWIR_1$) in DOY 184-201, 2005, at the Bartlett Experimental Forest flux tower site. PROSAIL-2 estimated surface reflectance come from forward simulation of the PROSAIL-2 model, which uses the mean values of inverted variables from inversion of the PROSAIL-2 model as input.

5.2. Comparison between retrieved and observed reflectances of MODIS daily data collection from DOY 184 to 201 in 2005

After inversion of the PROSAIL-2 model for the daily MODIS data collection (from DOY 184–201 in 2005), the mean values of the retrieved variable distributions were utilized as inputs to calculate the reflectances with forward simulations of the PROSAIL-2 model. Fig. 5 shows a comparison between PROSAIL-2 estimated reflectances and MODIS observed reflectances of the green, red, NIR_1, NIR_2, and $SWIR_1$ bands. The correlation coefficients between retrieved and observed MODIS visible reflectances are 0.92 for the green band and 0.93 for the red band, respectively. The root mean squared errors (RMSE) between observed and retrieved MODIS visible reflectances are 0.0023 for the green band and 0.0040 for the red band. The correlation coefficients between estimated and observed NIR to SWIR reflectances are 0.92, 0.89, and 0.90 for NIR_1, NIR_2 and $SWIR_1$, respectively. The RMSE between estimated and observed NIR to SWIR reflectances are 0.025, 0.025, and 0.016 for NIR_1, NIR_2 and $SWIR_1$, respectively. Note that the daily data collection spanned over a period of eighteen days, and any variation of leaf and canopy during the period may have contributed to the discrepancies between the PROSAIL-2 estimated reflectances and MODIS observed reflectances, although we would not expect large changes at both leaf and canopy levels because the canopy was fully developed during early July. Possible errors (e.g. imperfect atmospheric correction) introduced during the MODIS pre-processing may also contribute to the discrepancies. The comparison suggests that the PROSAIL-2 model with the retrieved mean values of individual variables reasonably reproduces the surface reflectances of the temperate deciduous broadleaf forest site.

5.3. Uncertainty of individual variables from inversion of the PROSAIL-2 model with MODIS daily data collection from DOY 184 to 201 in 2005

During the inversion of the PROSAIL-2 model, the Metropolis inversion algorithm estimated probability distributions for individual model variables. The posterior distributions offer a measure of uncertainty in the form of standard deviations or other quantile intervals, and the shapes of the distributions also provide a measure of compatibility between model and data. We examined the histograms of the sixteen variables from inversion of the PROSAIL-2 model for the MODIS data collection from DOY 184 to 201 in 2005, and simply ranked them into three categories: "well-constrained", "poorly-constrained" and "edge-hitting" (Braswell et al., 2005; Zhang et al., 2005). The "well-constrained" variables usually have well-defined distributions, with small standard deviations relative to their allowable ranges. The "poorly-constrained" variables have relatively flat distributions with large standard deviations relative to their allowable ranges. For the "edge-hitting" variables, their modes of retrieved values occur near one of the edges of their allowable ranges and most of the retrieved values were clustered near this edge. Figs. 6–10 showed the histograms of the sixteen variables in the PROSAIL-2 model and the histogram of leaf area index (LAI). Eight variables belong to the "well-constrained" category: plant area index (Fig. 6a), five leaf variables (leaf internal structure variable, leaf chlorophyll content, leaf brown pigment content, leaf dry matter

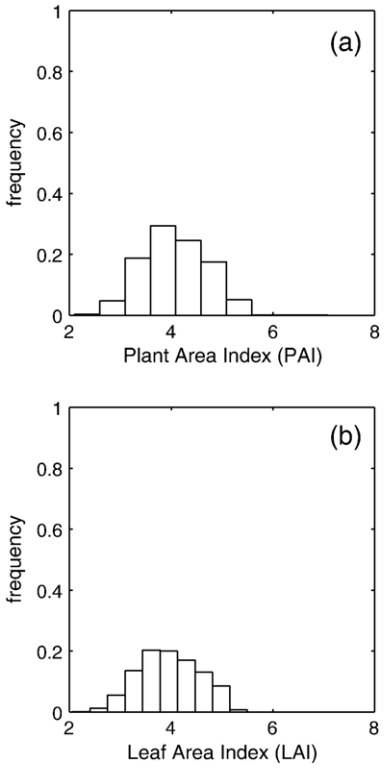

Fig. 6. Histograms of (a) plant area index (PAI) and (b) leaf area index (LAI) at the Bartlett Experimental Forest tower site, as estimated from inversion of the PROSAIL-2 model and MODIS data collection of DOY 184 to 201 in 2005.

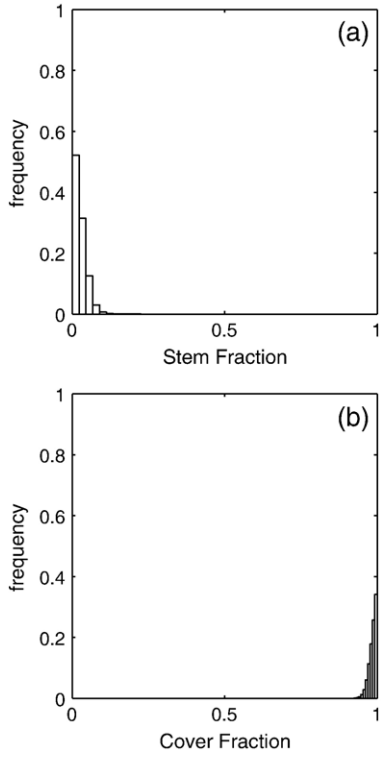

Fig. 7. Histograms of (a) stem fraction; (b) cover fraction at the Bartlett Experimental Forest tower site, as estimated from inversion of the PROSAIL-2 model and MODIS data collection of DOY 184 to 201 in 2005.

and leaf equivalent water thickness, Fig. 8), average leaf inclination angle and leaf BRDF effect variable (Fig. 9a and c). Six variables belong to the "poor-constrained" category: average stem inclination angle, stem BRDF effect variable (Fig. 9b and d), two soil variables and two stem variables in SAIL-2 model (Fig. 10). Stem fraction and cover fraction belong to the "edge-hitting" category (Fig. 7). Because stem fraction was distributed near zero and cover fraction was distributed near one, stem and soil had little effect on the canopy optical characteristics and consequently little information about stem and soil could be retrieved from MODIS observations of DOY 184–201, 2005. LAI was estimated using the equation LAI=(1-SFRAC)×PAI. LAI is also a well-constrained variable (Fig. 6b).

5.4. Distribution of $FAPAR_{canopy}$, $FAPAR_{leaf}$, and $FAPAR_{chl}$ using MODIS daily data collection from DOY 184 to 201 in 2005

We estimated the distributions of $FAPAR_{canopy}$, $FAPAR_{leaf}$, and $FAPAR_{chl}$ for the MODIS data collection from DOY 184 to 201 in 2005, using the retrieved distributions of individual variables in PROSAIL-2, and extracted their mean and standard deviation values (Fig. 11). The mean values of $FAPAR_{canopy}$, $FAPAR_{leaf}$, and $FAPAR_{chl}$ were 0.879, 0.858, and 0.707, respectively. The standard deviation values were 0.033, 0.035, and 0.026, respectively. $FAPAR_{canopy}$, $FAPAR_{leaf}$, and $FAPAR_{chl}$ were well-constrained variables.

The difference between $FAPAR_{canopy}$ and $FAPAR_{leaf}$ is attributed to light absorption by stem ($APAR_{stem}$), i.e., the non-leaf part of the canopy. During DOY 184 to 201 in 2005, the vegetation canopy is dominated by leaves, and only a very small proportion of stems are observed by the MODIS sensor. This may explain why the mean $FAPAR_{canopy}$ value is only slightly higher than the mean value of $FAPAR_{leaf}$. The difference between $FAPAR_{leaf}$ and $FAPAR_{chl}$ is attributed to light absorption by the non-chlorophyll component of the leaf. The mean $FAPAR_{chl}$ value is 15% lower than the mean value of $FAPAR_{leaf}$ and 17% lower than the mean value of $FAPAR_{canopy}$.

NDVI has been widely used for estimation of $FAPAR_{canopy}$ and gross and net primary production (GPP, NPP) of vegetation (Potter et al., 1993; Prince & Goward, 1995; Ruimy et al., 1996; Running et al., 2004). In recent years, EVI was generated as a standard product of MODIS Land Science Team (Justice et al., 1998). We calculated the mean and standard deviation of NDVI and EVI using the same MODIS images for the data collection from DOY 184 to 201 in 2005. The mean values of NDVI and EVI were 0.853 and 0.578, respectively. The standard deviations of NDVI and EVI were 0.010 and 0.073, respectively. The mean NDVI value is close to $FAPAR_{leaf}$, which supports the earlier studies that used NDVI to approximate $FAPAR_{canopy}$ (e.g., Goward & Huemmrich, 1992), as $FAPAR_{leaf}$ and $FAPAR_{canopy}$ values are close to each other. The mean EVI value is closer to the mean $FAPAR_{chl}$ values than to mean $FAPAR_{leaf}$. Note that reflectance values in daily MODIS images are not BRDF corrected reflectance; therefore, the observation viewing geometry has an effect on the ranges of NDVI and EVI values that are directly calculated from daily MODIS images.

6. Discussion

MODIS sensors on the Terra and Aqua platforms provide daily observations of the land surface at moderate spatial resolution (250m–1000m). MODIS has been used to monitor phenology (e.g., Xiao et al., 2004, 2005; Zhang et al., 2004a,b, 2003). However, there is a long and snowy winter season over temperate forest areas like Harvard Forest in MA, Howland Forest in ME, and Bartlett Experimental Forest in NH, USA. Through better screening out of the observations contaminated by snow and atmosphere, one can construct time series data for identifying green-up and leaf-off of forests more accurately (Figs. 2, 3 and 4). The plant growing season at the Bartlett flux tower site was from DOY 122 to 282 in 2004, approximately 160 days long. EVI values during the plant growing season was greater than 0.3. NDVI, EVI and LSWI had a rapid increase from DOY 122 to DOY 135, and also had a quick decrease after DOY 275 in 2004 at the tower site (Fig. 4h). The field measured daily $FAPAR_{canopy}$ and NDVI at the Bartlett Experimental Forest flux tower site in 2004 (unpublished data and they will be reported in another paper) shows similar green-up increase and leaf-senescence tendencies during the same periods. The MODIS measurements were consistent with field measurements.

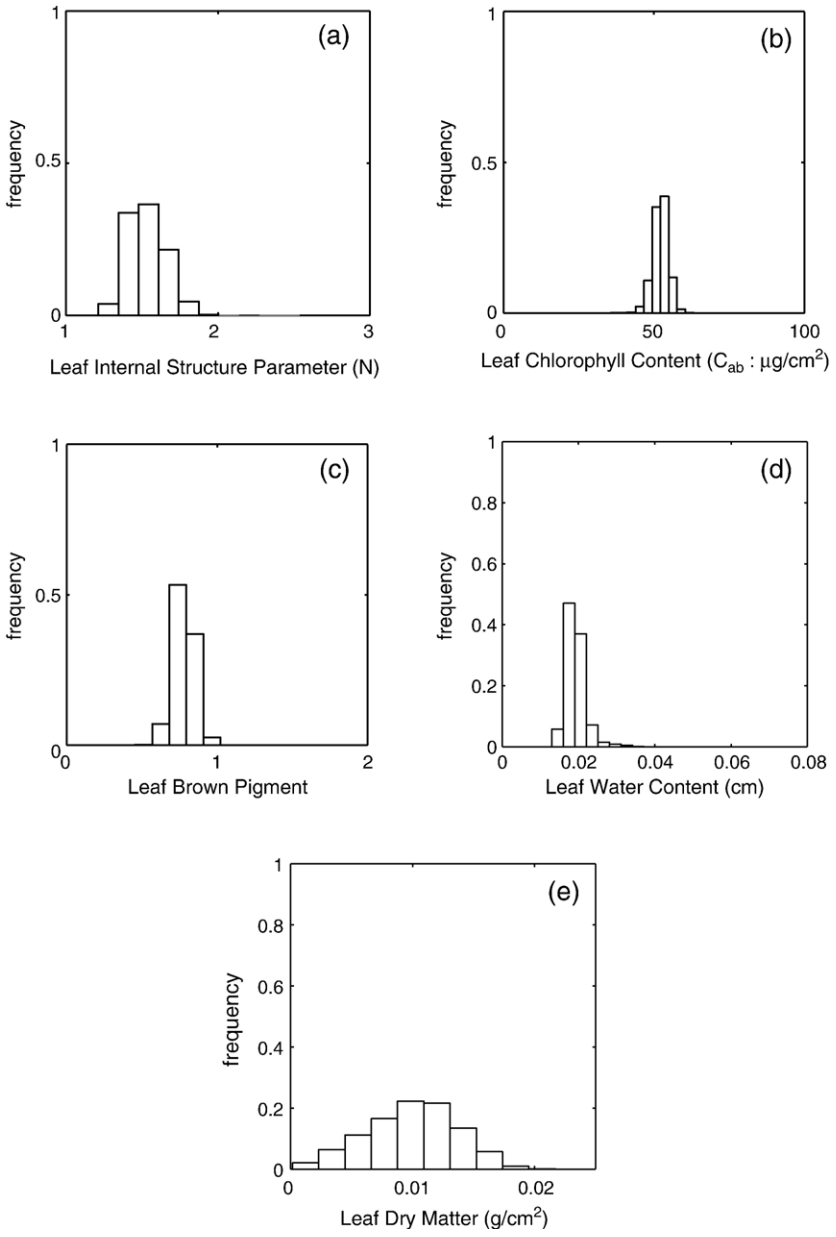

Fig. 8. Histograms of (a) leaf internal variable (N), (b) leaf chlorophyll content (C_{ab}, mg/cm2), (c) leaf brown pigment (C_{brown}), (d) leaf equivalent water thickness (C_w, cm); and (e) leaf dry matter (C_m, g/cm2) at the Bartlett Experimental Forest tower site, as estimated from inversion of the PROSAIL-2 model and MODIS data collection of DOY 184 to 201 in 2005.

A number of radiative transfer models have been used to retrieve LAI and estimate $FAPAR_{canopy}$ (e.g., Asner et al., 1998; Bicheron & Leroy, 1999; Myneni et al., 1997). The MODIS Land Science Team has used reflectance of MODIS red and NIR_1 bands as inputs to a 3-dimensional radiative transfer model to provide standard products of $FARAR_{canopy}$ and LAI at 1-km spatial resolution (Justice et al., 1998; Knyazikhin et al., 1998b, and personal communication with Dr. Ranga Myneni). The PROSAIL-2 model we used in this study is relatively simple in structure (one dimension in space) but complex in leaf biochemistry and spectral bands. The PROSAIL-2 model uses five MODIS spectral bands as input data. The Eqs. (5)–(6) used to simulate soil and stem reflectance in PROSAIL-2 are simple. As the results show that the retrieved cover fraction and stem fraction are "edge-hitting" and the retrieved reflectances and real MODIS reflectances match well, whether the formula of the soil and stem is simple or complex does not matter. That is to say, for this case, very little information could be retrieved from the real MODIS observations. For cases where there are significant soil or stem observed by MODIS, for example, sparse vegetation, one has chances to check whether the soil/stem equations are applicable and whether it is a need to develop more complex approaches to simulate soil/stem reflectances. There is also a need to further combine complex canopy radiative transfer models with leaf-level PROSPECT for future studies.

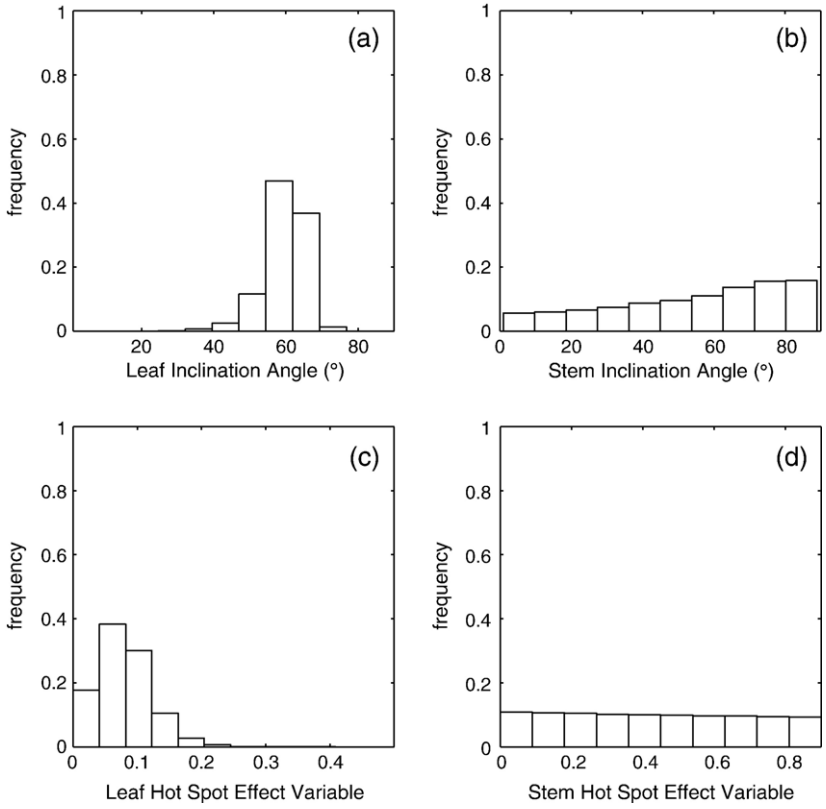

Fig. 9. Histograms of (a) average leaf inclination angle (degree), (b) average stem inclination angle (degree), (c) leaf BRDF effect variable (d) stem BRDF effect variable at the Bartlett Experimental Forest tower site, as estimated from inversion of the PROSAIL-2 model and MODIS data collection of DOY 184 to 201 in 2005.

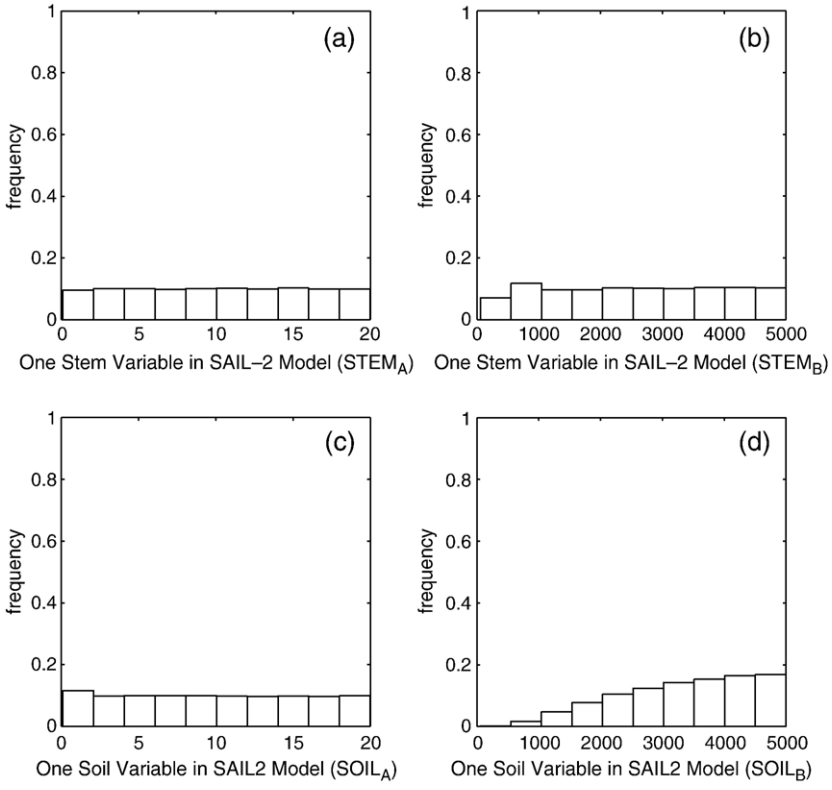

Fig. 10. Histograms of (a) one stem variable ($STEM_A$); (b) one stem variable ($STEM_B$); (c) one soil variable ($SOIL_A$); (d) one soil variable ($SOIL_B$) at the Bartlett Experimental Forest tower site, as estimated from inversion of the PROSAIL-2 model and MODIS data collection of DOY 184 to 201 in 2005.

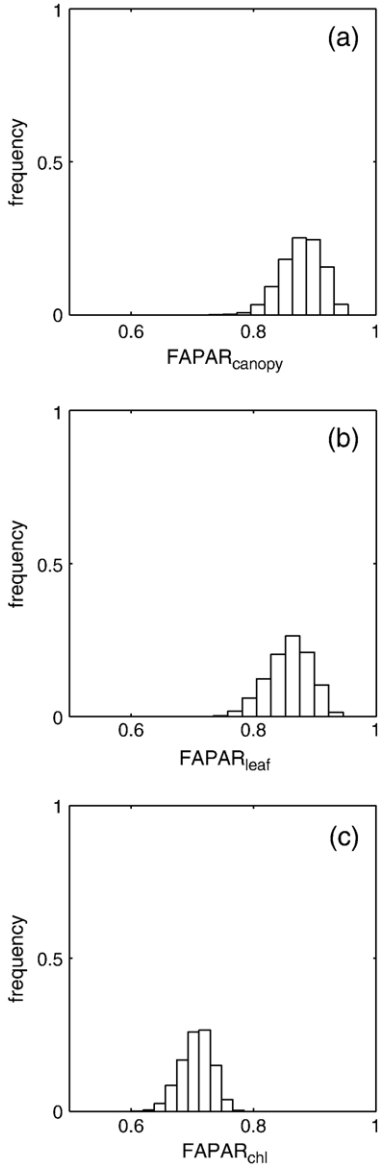

Fig. 11. Histograms of the fraction of photosynthetically active radiation absorbed by (a) canopy (FAPAR$_{canopy}$), (b) by leaf (FAPAR$_{leaf}$) and (c) by chlorophyll (FAPAR$_{chl}$) at the Bartlett Experimental Forest tower site, as estimated from forward simulation of the PROSAIL-2 model and MODIS data collection of DOY 184 to 201 in 2005.

Very limited amount of *in situ* data at both canopy and leaf levels, which can be used for evaluation of biophysical/biochemical variables at moderate (500 m to 1000 m) spatial resolution, have been collected because of expensive financial and human resource cost (e.g., Cohen et al., 2003; Turner et al., 2003). Here we discuss four variables (LAI, leaf dry matter, leaf chlorophyll content and FAPAR$_{canopy}$) that are important for interpreting the results of inversion of the PROSAIL-2 model in this study. The inversion of the PROSAIL-2 model estimated LAI with a mean of 3.99 and a standard deviation of 0.66. The field measured LAI around the footprint of the Bartlett Experimental Forest flux tower site during the peak growing season in 2004 varied between 3.6 and 5.1 m^2/m^2 (Smith et al. unpublished data). The model-based estimation of LAI overlapped with the range of field measured LAI. Leaf dry matter (C_m, g/cm^2), another widely used variable in biogeochemical models, had a mean of 0.0105 g/cm^2 and standard deviation of 0.0041 g/cm^2. The top-canopy leaf specific weight used for the deciduous trees in the Bartlett Experimental Forest by Ollinger and Smith (2005) was 0.01 g/cm^2, which was very close to the model-based estimate of the mean value of leaf dry matter. The histogram of inverted leaf chlorophyll content has a mean of 52.3 μg/cm^2 and standard deviation of 2.6 μg/cm^2. The field measured leaf chlorophyll content for the leaves of mid to upper canopy of the deciduous species in early July of 2005 has a range of 23.5–52.6 μg/cm^2. The range of inverted leaf chlorophyll content overlapped with the range of field measurements. Field measured leaf chlorophyll content for top, middle and bottom leaves of forest canopy are proposed to be conducted in the future. We suspect MODIS observed leaf chlorophyll content is closer to top-leaf chlorophyll content than to middle-leaf and bottom-leaf contents. The model-based FAPAR$_{canopy}$ (Fig. 11) had a range from 0.72 to 0.95 (most in the range from 0.77 to 0.95). The FAPAR$_{canopy}$ calculated from field measurements of radiation above- and below-canopy at the Bartlett Experimental Forest flux tower site, had a range from 0.798 to 0.930 during 11:00 am to 1:00 pm of DOY 184 to 201 in 2005. The range of field measured FAPAR$_{canopy}$ falls within the inverted range of FAPAR$_{canopy}$, although the field radius is 15 m and the MODIS pixel has a spatial resolution of 500 m. We may estimate canopy/leaf variables for some whole snow-free growing season and conduct field canopy/leaf measurement during the same period in the future when we have enough financial and human resources. Then we may check how canopy/leaf variables change over the snow-free growing season and to evaluate the capability of the inversion procedure that if it can catch up the seasonal status of canopy/leaf.

The results of this study, together with the results from our previous study (Zhang et al., 2005) highlight the substantial difference between FAPAR$_{canopy}$ and FAPAR$_{chl}$ for the two temperate deciduous broadleaf forests (the Harvard Forest and the Bartlett Experimental Forest). The results suggest that the Production Efficiency Models (e.g., Potter et al., 1993; Prince & Goward, 1995; Ruimy et al., 1996; Running et al., 2004) that use FAPAR$_{canopy}$ to estimate the amount of PAR for photosynthesis may potentially overestimate amount of light absorption for photosynthesis, an important source of uncertainty for calculation of GPP and NPP.

In summary, this study provides an improved procedure for selecting atmosphere-contamination and snow-contamination-free MODIS observations. With a contamination-free (atmospheric-contamination-free and/or snow-contamination-free) time series of daily MODIS observations, the seasonal variations of NDVI, EVI, LSWI and snow cover fraction of a temperate deciduous broadleaf forest site is better interpreted through the seasonal dynamics of surface reflectance of MODIS seven spectral bands. The procedure

can be tested at other places. This study continued to evaluate an innovative methodology presented in our previous study (Zhang et al., 2005) that combined radiative transfer model with the Metropolis statistical method to estimate leaf- and canopy-level biophysical/biochemical properties of the forests. It has clearly demonstrated the potential of daily MODIS data at 500-m spatial resolution for better characterization of forests. This study further strengthens our call for routine field measurements of canopy-level variables (e.g., LAI) and leaf-level variables (e.g., chlorophyll, other pigments, leaf dry matter, and leaf water content), the resultant data could shed new insight for better understanding of the seasonal dynamics of leaf and canopy.

Acknowledgements

We would like to thank Dr. Marvin E. Bauer and the anonymous referees whose careful reviews resulted in a more meaningful analysis and a much improved manuscript. The study was supported by NASA Earth System Science Graduate Fellowship (NGT5-30477 for Q. Zhang), NASA Earth Observation System Interdisciplinary Science project (NAG5-10135) and NASA Carbon Cycle Science Project (CARBON-0000-1234). Field data of the study site are from the long-term research studies at the Bartlett Experimental Forest under the support of the U.S. Department of Agriculture, Forest Service, Northeastern Research Station.

References

Andrieu, B., Baret, F., Jacquemoud, S., Malthus, T., & Steven, M. (1997). Evaluation of an improved version of SAIL model for simulating bidirectional reflectance of sugar beet canopies. *Remote Sensing of Environment*, *60*, 247−257.

Arora, V. K. (2002). Modeling vegetation as a dynamic component in soil-vegetation-atmosphere transfer schemes and hydrological models. *Reviews of Geophysics*, *40*.

Asner, G. P., Wessman, C. A., & Archer, S. (1998). Scale dependence of absorption of photosynthetically active radiation in terrestrial ecosystems. *Ecological Applications*, *8*, 1003−1021.

Bacour, C., Jacquemoud, S., Leroy, M., Hautecoeur, O., Weiss, M., Prevot, L., et al. (2002). Reliability of the estimation of vegetation characteristics by inversion of three canopy reflectance models on airborne POLDER data. *Agronomie*, *22*, 555−565.

Badhwar, G. D., Verhoef, W., & Bunnik, N. J. J. (1985). Comparative-study of SUITS and SAIL canopy reflectance models. *Remote Sensing of Environment*, *17*, 179−195.

Baret, F., & Fourty, T. (1997). Radiometric estimates of nitrogen status in leaves and canopies. In G. Lemaire (Ed.), *Diagnosis of the nitrogen status in crops* (pp. 201−227). Berlin: Springer.

Bicheron, P., & Leroy, M. (1999). A method of biophysical parameter retrieval at global scale by inversion of a vegetation reflectance model. *Remote Sensing of Environment*, *67*, 251−266.

Braswell, B. H., Jr. (1996). Global terrestrial biogeochemistry: Perturbations, interactions and time scales. Ph.D., Earth Sciences, University of New Hampshire, Durham, New Hampshire.

Braswell, B. H., Sacks, W. J., Linder, E., & Schimel, D. S. (2005). Estimating diurnal to annual ecosystem parameters by synthesis of a carbon flux model with eddy covariance net ecosystem exchange observations. *Global Change Biology*, *11*, 335−355.

Braswell, B. H., Schimel, D. S., Privette, J. L., Moore, B., Emery, W. J., Sulzman, E. W., et al. (1996). Extracting ecological and biophysical information from AVHRR optical data: An integrated algorithm based on inverse modeling. *Journal of Geophysical Research-Atmospheres*, *101*, 23335−23348.

Cohen, W. B., Maiersperger, T. K., Yang, Z. Q., Gower, S. T., Turner, D. P., Ritts, W. D., et al. (2003). Comparisons of land cover and LAI estimates derived from ETM plus and MODIS for four sites in North America: A quality assessment of 2000/2001 provisional MODIS products. *Remote Sensing of Environment*, *88*, 233−255.

Combal, B., Baret, F., & Weiss, M. (2002). Improving canopy variables estimation from remote sensing data by exploiting ancillary information. Case study on sugar beet canopies. *Agronomie*, *22*, 205−215.

Defries, R. S., Houghton, R. A., Hansen, M. C., Field, C. B., Skole, D., & Townshend, J. (2002). Carbon emissions from tropical deforestation and regrowth based on satellite observations for the 1980s and 1990s. *Proceedings of the National Academy of Sciences of the United States of America*, *99*, 14256−14261.

Demarez, V., Gastellu-Etchegorry, J. P., Mougin, E., Marty, G., Proisy, C., Dufrene, E., et al. (1999). Seasonal variation of leaf chlorophyll content of a temperate forest. Inversion of the PROSPECT model. *International Journal of Remote Sensing*, *20*, 879−894.

Di Bella, C. M., Paruelo, J. M., Becerra, J. E., Bacour, C., & Baret, F. (2004). Effect of senescent leaves on NDVI-based estimates of f APAR: Experimental and modelling evidences. *International Journal of Remote Sensing*, *25*, 5415−5427.

Fitzjarrald, D. R., Acevedo, O. C., & Moore, K. E. (2001). Climatic consequences of leaf presence in the eastern United States. *Journal of Climate*, *14*, 598−614.

Gelman, A., Carlin, J. B., Stern, H. S., & Rubin, D. B. (2000). Markov chain simulation (chapter 11). *Bayesian data analysis* New York: Champman and Hall/CRC.

Gitelson, A., Stark, R., Grits, U., Rundquist, D., Kaufman, Y., & Derry, D. (2002). Vegetation and soil lines in visible spectral space: A concept and technique for remote estimation of vegetation fraction. *International Journal of Remote Sensing*, *23*, 2537−2562.

Gobron, N., Pinty, B., Verstraete, M. M., & Widlowski, J. L. (2000). Advanced vegetation indices optimized for up-coming sensors: Design, performance, and applications. *IEEE Transactions on Geoscience and Remote Sensing*, *38*, 2489−2505.

Gobron, N., Pinty, B., Verstraete, M. M., Widlowski, J. L., & Diner, D. J. (2002). Uniqueness of multiangular measurements: — Part II. Joint retrieval of vegetation structure and photosynthetic activity from MISR. *IEEE Transactions on Geoscience and Remote Sensing*, *40*, 1574−1592.

Goel, N. S., & Deering, D. W. (1985). Evaluation of a canopy reflectance model for LAI estimation through its inversion. *IEEE Transactions on Geoscience and Remote Sensing*, *23*, 674−684.

Goel, N. S., & Thompson, R. L. (1984). Inversion of vegetation canopy reflectance models for estimating agronomic variables: 5. Estimation of leaf-area index and average leaf angle using measured canopy reflectances. *Remote Sensing of Environment*, *16*, 69−85.

Gond, V., De Pury, D. G. G., Veroustraete, F., & Ceulemans, R. (1999). Seasonal variations in leaf area index, leaf chlorophyll, and water content; scaling-up to estimate fAPAR and carbon balance in a multilayer, multispecies temperate forest. *Tree Physiology*, *19*, 673−679.

Goward, S. N., & Huemmrich, K. F. (1992). Vegetation canopy PAR absorptance and the normalized difference vegetation index — An assessment using the SAIL model. *Remote Sensing of Environment*, *39*, 119−140.

Goward, S. N., & Prince, S. D. (1995). Transient effects of climate on vegetation dynamics: Satellite observations. *Journal of Biogeography*, *22*, 549−564.

Huete, A. R., Hua, G., Qi, J., Chehbouni, A., & Vanleeuwen, W. J. D. (1992). Normalization of multidirectional red and NIR reflectances with the SAVI. *Remote Sensing of Environment*, *41*, 143−154.

Huete, A. R., Liu, H. Q., Batchily, K., & Vanleeuwen, W. (1997). A comparison of vegetation indices global set of TM images for EOS-MODIS. *Remote Sensing of Environment*, *59*, 440−451.

Hurtt, G. C., & Armstrong, R. A. (1996). A pelagic ecosystem model calibrated with BATS data. *Deep-Sea Research: Part 2. Topical Studies in Oceanography*, *43*, 653−683.

Jacquemoud, S., Bacour, C., Poilve, H., & Frangi, J. P. (2000). Comparison of four radiative transfer models to simulate plant canopies reflectance: Direct and inverse mode. *Remote Sensing of Environment*, *74*, 471−481.

Jacquemoud, S., & Baret, F. (1990). PROSPECT — A model of leaf optical-properties spectra. *Remote Sensing of Environment*, *34*, 75−91.

Jacquemoud, S., Ustin, S. L., Verdebout, J., Schmuck, G., Andreoli, G., & Hosgood, B. (1996). Estimating leaf biochemistry using the PROSPECT leaf optical properties model. *Remote Sensing of Environment*, *56*, 194−202.

Justice, C. O., Vermote, E., Townshend, J. R. G., Defries, R., Roy, D. P., Hall, D. K., et al. (1998). The Moderate Resolution Imaging Spectro-radiometer (MODIS): Land remote sensing for global change research. *IEEE Transactions on Geoscience and Remote Sensing*, *36*, 1228−1249.

Kaufman, Y., Kleidman, R., Hall, D., Martins, J., & Barton, J. (2002). Remote sensing of subpixel snow cover using 0.66 and 2.1 mm channels. *Geophysical Research Letters*, *29*.

Knyazikhin, Y., Martonchik, J. V., Diner, D. J., Myneni, R. B., Verstraete, M., Pinty, B., et al. (1998a). Estimation of vegetation canopy leaf area index and fraction of absorbed photosynthetically active radiation from atmosphere-corrected MISR data. *Journal of Geophysical Research-Atmospheres*, *103*, 32239−32256.

Knyazikhin, Y., Martonchik, J. V., Myneni, R. B., Diner, D. J., & Running, S. W. (1998b). Synergistic algorithm for estimating vegetation canopy leaf area index and fraction of absorbed photosynthetically active radiation from MODIS and MISR data. *Journal of Geophysical Research-Atmospheres*, *103*, 32257−32275.

Kodani, E., Awaya, Y., Tanaka, K., & Matsumura, N. (2002). Seasonal patterns of canopy structure, biochemistry and spectral reflectance in a broad-leaved deciduous Fagus crenata canopy. *Forest Ecology and Management*, *167*, 233−249.

Kuusk, A. (1985). The hotspot effect of a uniform vegetative cover. *Soviet Journal of Remote Sensing*, *3*, 645−658.

Lawrence, D. M., & Slingo, J. M. (2004). An annual cycle of vegetation in a GCM: Part II. Global impacts on climate and hydrology. *Climate Dynamics*, *22*, 107−122.

Linderman, M., Rowhani, P., Benz, D., Serneels, S., & Lambin, E. F. (2005). Land-cover change and vegetation dynamics across Africa. *Journal of Geophysical Research-Atmospheres*, *110*.

Lovell, J. L., & Graetz, R. D. (2001). Filtering pathfinder AVHRR land NDVI data for Australia. *International Journal of Remote Sensing*, *22*, 2649−2654.

Major, D. J., Schaalje, G. B., Wiegand, C., & Blad, B. L. (1992). Accuracy and sensitivity analyses of SAIL model-predicted reflectance of maize. *Remote Sensing of Environment*, *41*, 61−70.

Metropolis, N., Rosenbluth, A. W., Rosenbluth, M. N., Teller, A. H., & Teller, E. (1953). Equations of state calculations by fast computing machines. *Journal of Chemical Physics*, *21*, 1087−1092.

Myneni, R. B., Hoffman, S., Knyazikhin, Y., Privette, J. L., Glassy, J., Tian, Y., et al. (2002). Global products of vegetation leaf area and fraction absorbed PAR from year one of MODIS data. *Remote Sensing of Environment*, *83*, 214−231.

Myneni, R. B., Nemani, R. R., & Running, S. W. (1997). Estimation of global leaf area index and absorbed PAR using radiative transfer models. *IEEE Transactions on Geoscience and Remote Sensing*, *35*, 1380−1393.

Ollinger, S., & Smith, M. L (2005). Net Primary Production and Canopy Nitrogen in a Temperate Forest Landscape: an Analysis Using Imaging Spectroscopy, Modeling and Field Data. *Ecosystems*, *8*, 760−778.

Osborne, T. M., Lawrence, D. M., Slingo, J. M., Challinor, A. J., & Wheeler, T. R. (2004). Influence of vegetation on the local climate and hydrology in the tropics: Sensitivity to soil parameters. *Climate Dynamics*, *23*, 45−61.

Pettorelli, N., Vik, J. O., Mysterud, A., Gaillard, J. -M., Tucker, C. J., & Stenseth (2005). Using the satellite-derived NDVI to assess ecological responses to environmental change. *Trends in Ecology and Evolution*, *20*, 503−510.

Pielke, R. A., Avissar, R., Raupach, M., Dolman, A. J., Zeng, X. B., & Denning, A. S. (1998). Interactions between the atmosphere and terrestrial ecosystems: Influence on weather and climate. *Global Change Biology*, *4*, 461−475.

Potter, C. S., Randerson, J. T., Field, C. B., Matson, P. A., Vitousek, P. M., Mooney, H. A., et al. (1993). Terrestrial ecosystem production — A process model-based on global satellite and surface data. *Global Biogeochemical Cycles*, *7*, 811−841.

Prince, S. D., & Goward, S. N. (1995). Global primary production: A remote sensing approach. *Journal of Biogeography*, *22*, 815−835.

Prince, S. D., & Goward, S. N. (1996). Evaluation of the NOAA/NASA pathfinder AVHRR land data set for global primary production modelling. *International Journal of Remote Sensing*, *17*, 217−221.

Qin, W. (1993). Modeling bidirectional reflectance of multicomponent vegetation canopies. *Remote Sensing of Environment*, *46*, 235−245.

Remer, L., Wald, A., & Kaufman, Y. (2001). Angular and seasonal variation of spectral surface reflectance ratios: Implications for the remote sensing of aerosol over land. *IEEE Transactions on Geoscience and Remote Sensing*, *39*, 275−283.

Richardson, A. D., & Berlyn, G. P. (2002). Spectral reflectance and photosynthetic properties of *Betula papyrifera* (Betulaceae) leaves along an elevational gradient on Mt. Mansfield, Vermont, USA. *American Journal of Botany*, *89*, 88−94.

Richardson, A. D., Berlyn, G. P., & Duigan, S. P. (2003). Reflectance of Alaskan black spruce and white spruce foliage in relation to elevation and latitude. *Tree Physiology*, *23*, 537−544.

Ruimy, A., Dedieu, G., & Saugier, B. (1996). TURC: A diagnostic model of continental gross primary productivity and net primary productivity. *Global Biogeochemical Cycles*, *10*, 269−285.

Running, S., Nemani, R., Heinsch, F., Zhao, M., Reeves, M., & Hashimoto, H. (2004). A continuous satellite-derived measure of global terrestrial primary production. *Bioscience*, *54*, 547−560.

Stylinski, C. D., Gamon, J. A., & Oechel, W. C. (2002). Seasonal patterns of reflectance indices, carotenoid pigments and photosynthesis of evergreen chaparral species. *Oecologia*, *131*, 366−374.

Taberner, M., Gobron, N., Melin, F., Pinty, B., & Verstraete, M. (2002). *The STARS FAPAR algorithm: A consolidated and generalized software package.* EUR Report No 20145 EN. Italy: Joint Research Center.

Tucker, C. J. (1979). Red and photographic infrared linear combinations for monitoring vegetation. *Remote Sensing of Environment*, *8*, 127−150.

Turner, D. P., Ritts, W. D., Cohen, W. B., Gower, S. T., Zhao, M. S., Running, S. W., et al. (2003). Scaling Gross Primary Production (GPP) over boreal and deciduous forest landscapes in support of MODIS GPP product validation. *Remote Sensing of Environment*, *88*, 256−270.

Ustin, S. L., Duan, L., & Hart, Q. J. (1994). Seasonal changes observed in AVIRIS images of Jasper Ridge, California. *Proceedings International Geoscience and Remote Sensing Symposium IGARSS '94*.

Verhoef, W. (1984). Light-scattering by leaf layers with application to canopy reflectance modeling — The SAIL model. *Remote Sensing of Environment*, *16*, 125−141.

Verhoef, W. (1985). Earth observation modeling based on layer scattering matrices. *Remote Sensing of Environment*, *17*, 165−178.

Verhoef, W., & Bach, H. (2003). Simulation of hyperspectral and directional radiance images using coupled biophysical and atmospheric radiative transfer models. *Remote Sensing of Environment*, *87*, 23−41.

Wang, Y. (2002). Assesment of the MODIS LAI and FPAR algorithm: Retrieval quality, theoretical basis and validation. Ph.D., Geography, Boston University, Boston.

Weiss, M., Baret, F., Myneni, R. B., Pragnere, A., & Knyazikhin, Y. (2000). Investigation of a model inversion technique to estimate canopy biophysical variables from spectral and directional reflectance data. *Agronomie*, *20*, 3−22.

Xiao, X. M., Zhang, Q. Y., Braswell, B., Urbanski, S., Boles, S., Wofsy, S., et al. (2004). Modeling gross primary production of temperate deciduous broadleaf forest using satellite images and climate data. *Remote Sensing of Environment*, *91*, 256−270.

Xiao, X. M., Zhang, Q. Y., Saleska, S., Hutyra, L., Camargo, P. D., Wofsy, S., et al. (2005). Satellite-based modeling of gross primary production in a seasonally moist tropical evergreen forest. *Remote Sensing of Environment*, *94*, 105−122.

Zarco-Tejada, P. J., Rueda, C. A., & Ustin, S. L. (2003). Water content estimation in vegetation with MODIS reflectance data and model inversion methods. *Remote Sensing of Environment*, *85*, 109−124.

Zhang, X. Y., Friedl, M. A., Schaaf, C. B., & Strahler, A. H. (2004a). Climate controls on vegetation phenological patterns in northern mid- and high latitudes inferred from MODIS data. *Global Change Biology*, *10*, 1133−1145.

Zhang, X. Y., Friedl, M. A., Schaaf, C. B., Strahler, A. H., Hodges, J. C. F., Gao, F., et al. (2003). Monitoring vegetation phenology using MODIS. *Remote Sensing of Environment*, *84*, 471−475.

Zhang, X. Y., Friedl, M. A., Schaaf, C. B., Strahler, A. H., & Schneider, A. (2004b). The footprint of urban climates on vegetation phenology. *Geophysical Research Letters*, *31*.

Zhang, Q. Y., Xiao, X. M., Braswell, B., Linder, E., Baret, F., & Moore, B. (2005). Estimating light absorption by chlorophyll, leaf and canopy in a deciduous broadleaf forest using MODIS data and a radiative transfer model. *Remote Sensing of Environment*, *99*, 357−371.